

BRDF measurement of understory vegetation in pine forests: dwarf shrubs, lichen, and moss

Jouni I. Peltoniemi^{a,*}, Sanna Kaasalainen^a, Jyri Näränen^{a,b}, Miina Rautiainen^b,
Pauline Stenberg^b, Heikki Smolander^c, Sampo Smolander^d, Pekka Voipio^c

^a*Finnish Geodetic Institute, Finland*

^b*University of Helsinki, Finland*

^c*Finnish Forest Research Institute, Finland*

^d*Division of Atmospheric Sciences, University of Helsinki, Finland*

Received 28 July 2004; received in revised form 8 October 2004; accepted 8 October 2004

Abstract

The spectral and directional reflection properties of pine forest understory in Suonenjoki, Finland were measured using a newly developed transportable field goniospectrometer under direct sunlight or plant lamp. The samples represent the most typical types in Finnish forests. Large differences between species were found. Wax-leaved shrubs such as lingonberry and blueberry proved to be strong forward scatterers, whereas lichen and soft-leaved dwarf shrubs such as heather were strong backscatterers. The measured moss showed both forward and backscattering features. There were variations among the samples of the same species, but many typical features appeared consistent and reproducible. Both “pure” and mixed samples were measured, the latter showing smoother behavior than the former, that is, the strongest forward and backward features are downscaled. The results provide a starting point for an empirical understory model and a basis for development and validation of a theoretical model.

© 2004 Elsevier Inc. All rights reserved.

Keywords: BRDF; Spectrum; Goniometry; Radiative transfer; Remote sensing; Forest; Understory

1. Introduction

In typical remote sensing applications, the sensor receives a signal from both the target and its environment. In the case of forest remote sensing, there are less desired signals from the atmosphere and the forest floor (soil and/or understory vegetation). The separation of atmospheric effects as well as the influence of soil have been a subject of extensive studies (Huete (1989); Kaufman (1989); and references therein), but fewer investigators have dealt with the understory, although differences in understory composition are known to have a significant effect on the forest reflectance (Chen & Cihlar 1996; Spanner et al., 1990).

In the boreal zone, understory vegetation is like a miniature forest: its scattering properties are determined by the optical properties of leaves, their orientation, and spatial distribution (canopy structure), not to forget the underlying soil, litter horizon, and topography (Kuusk, 2001). The understory, however, is more compact and yet structurally more complex due to a larger species variation than the overstory.

The scattering properties of leaves are determined by factors such as chlorophyll and water content, internal structure, and surface properties (Walter-Shea & Norman 1991). In addition, their scattering function depends on leaf orientation with respect to the direction of illumination. As a result, leaves oriented towards the sun, for example, exhibit stronger backscattering than leaves turned away from the sun.

In natural conditions, the understory is more or less covered by the overstory. Overstory canopy structure (e.g.,

* Corresponding author. Tel.: +358 9 29555212.

E-mail address: jouni.peltoniemi@fgi.fi (J.I. Peltoniemi).

the orientation, spatial distribution, and density of leaves) modifies the directional distribution of light incident on the understory. It also affects the size and angular range of the visible understory in remotely sensed images, which has implications on the hot spot effect, for example.

Accurate models of understory reflectance are needed to separate the spectral signal from the background (understory) from that of the forest canopy (overstory), which is the target in many remote sensing applications. The models should be able to explain and predict the directional and spectral signatures or the bidirectional reflectance distribution functions (BRDF) of the vegetation (Hapke, 1993; Liang, 2004). Modeling of understory reflectance and especially models suitable for the complex mixed understory of boreal forests (e.g., Kuusk (2001)) are still in their infancy, although development of scattering models for leaves (e.g., Dawson et al. (1998); Ganapol et al. (1998); Jacquemoud and Baret (1990)), forest canopies (e.g., Kuusk and Nilson (2000), Li et al. (1995); North (1996), Widlowski et al. (2001)), and soils (Jacquemoud et al., 1992) has been going on actively for the past 20 years.

A prerequisite for adequate understory BRDF modeling is a large supply of empirical data which are scarce at the moment, especially for the boreal zone. BRDFs can be measured using goniometers (Bonnetfoy et al., 2000; Brissaud et al., 2004; Bruegge et al., 2000; Demircan et al., 2000; Hosgood et al., 2000; Sandmeier & Itten, 1999). So far, the BRDFs of primarily open vegetation, soil, and snow have been measured (Kuusk, 1991; Strub et al., 2003). A large number of BRDF measurements exists for lichen and moss (Solheim et al., 2000), and spectrometry for various understory, lichen, and moss species (Lang et al., 2002; Rees & Tutubalina, 2004) has also been made.

The BRDF is defined as the ratio of the reflected intensity $I(\mu, \phi)$ to incident unidirectional flux $F_0(\mu_0, \phi_0)$ as (Hapke, 1993; Liang, 2004)

$$R(\mu, \mu_0, \phi, \phi_0) = \frac{I(\mu, \phi)}{\mu_0 F_0(\mu_0, \phi_0)}, \quad (1)$$

where the angles are defined in Fig. 1. Because of phototropism and topography, vegetation is usually anisotropic requiring all the four angles, but it is here assumed for simplicity that most azimuthal effects are described by the difference $\phi - \phi_0$ and leave more detailed research for future.

The Finnish Geodetic Institute has developed several field goniometry systems for measuring the BRDF. The goniospectrometers have already been used, e.g., for measuring the BRDF of snow (Peltoniemi et al., submitted for publication). Our long-term goal is to measure BRDFs of the most common understory species in Finland and to create a spectral data bank. The first objective is to have a satisfactory characterization of the BRDFs of various species to be used for background modeling in forest scattering models, i.e., to help separate the signals from the tree canopy and understory. The next goal is to acquire

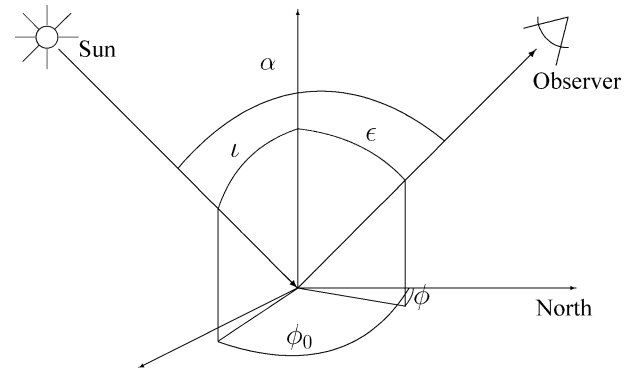


Fig. 1. The measurement geometry: $\mu = \cos \epsilon$ and $\mu_0 = \cos \iota$ are the zenith cosines of the emergent (observer) and incident (solar) radiation, respectively. ϕ and ϕ_0 are the corresponding azimuths. The phase or backscattering angle α is the angle between the observer and the sun. The principal plane is fixed by solar direction and surface normal, while the cross plane is a vertical plane, perpendicular to the principal plane.

accurate enough BRDFs to be used for identification of species and their abundance from remote sensing data. Empirical BRDF data to support the development and validation of physical scattering models of vegetation will be provided.

In this paper, BRDF measurements made in central Finland for seven common understory species are reported. First, the new implementation of the measurement technique and equipment is described, and then the results from the spectra measured during the campaign are discussed.

2. Material and methods

2.1. Site description

The study site was located near Suonenjoki Research Station (62°39N, 27°05E) of the Finnish Forest Research Institute. The whole area is Scots-pine (*Pinus sylvestris* L.)-dominated, and the site type according to the Cajanderian system (Cajander, 1909) ranged from CT (*Calluna vulgaris* L.), VT (*Vaccinium vitis-idaea* L.), to MT (*Vaccinium myrtillus* L.), which are the typical sites for Scots pine in Finland. Typical understory vegetation in the area included crowberry (*Empetrum nigrum* L.), several lichen species (*Cladonia* sp. and *Cladonia* sp.), and mosses (e.g., *Dicranum polysetum* Sw.).

2.2. Instrumentation

The BRDFs (Fig. 1) were measured using the transportable field goniometer of the Finnish Geodetic Institute, serial number 3 (Fig. 2). The spectra were recorded using ASD Field Spec PRO FR field spectrometer, with a useful range of 350 to 2350 nm in this setup. The field of view was 3°, and the footprint diameter was about 10 cm at nadir, elongating with larger zenith angles. Only the fore optics was mounted in the goniometer, and light was guided down



Fig. 2. Measurements being taken in Suonenjoki.

to the spectrometer using a 4-m-long optical fiber. The spectrometer itself had three separate sensors for wavelengths 350 to about 990, 990 to 1760, and 1760 to 2500 nm. Because of the construction, the footprints of these sensors had only partial alignment, that is, each one saw a slightly different area (10% to 30%). The design of the goniometer was robust. It consisted of two horizontally mounted rings of 2 m diameter, the one on top rotating 360° azimuthally and an arch of 220 cm radius, which was tilted to (0°,70°) angle range. The arch was supported by a mechanical winch with no motorized parts. Thus, it was weatherproof and tolerated rough transport and handling. It

weighed 150 kg and was transported using a light trailer. The drawbacks of the design were long mounting time (about 1 h), laborious operation (which needed 2–3 persons), and a few unmeasurable angles, e.g., around backscattering direction, which were shaded by the instrument itself.

For artificial illumination, a light source HMW 1200 (Ludvig Pani, Austria) was used, with a 1200 W metallogen lamp (DAYMAX DMI 1200, CA, USA), originally designed to simulate sunlight for plants. The spectrum had some spikes at some wavelengths, which disturbed the spectroscopy because the instrument had to be optimized for the brightest peaks, making dimmer bands rather dim. Increasing the integration time mostly solved the problem, except that the range 2350–2500 nm was unusable. The illumination pattern was homogeneous only in the center of the beam (10% drop at half width) but dropped below 50% at the limb. At 5-m illumination distance, the size of the spot was about 1 m, and the homogeneous area was 50 cm in diameter. With a flat target, that was not a problem because the detector footprint was 10 cm, but the present targets were 10–30 cm of height, which, together with the elongation at off-nadir angles, caused some error.



Fig. 3. Lichen and moss samples.

Table 1
All BRDF measurements made in Suonenjoki 2003

Target	Date	Light	No. of spectra
Lichen	12.8.	lamp 38°	126
Lichen	12.8.	lamp 48°	78
Lichen	13.8.	sun 62°	26
Moss	13.8.	Lamp 48°	58
Moss	13.8.	Lamp 35°	49
Crowberry	14.8.	Lamp 51°	74
Crowberry	14.8.	Lamp 56°	68
Heather 1	15.8.	Lamp 50°	71
Heather 1	15.8.	Lamp 41°	67
Heather 1	18.8.	Lamp 40°	79
Heather 2	19.8.	sun 51°	120
Lingonberry	20.8.	Lamp 59°	88
Lingonberry	20.8.	Lamp 42°	70
Blueberry	20.8.	Lamp 42°	74
Blueberry	20.8.	Lamp 58°	68
Mixed	21.8.	Lamp 59°	361

Name of the target, date of measurement, and light source used in the measurements (Sun/Lamp) and number of spectra taken.

An adjustable lightstand was built, allowing about 30° to 60° angles of illumination, depending on the terrain and space. A large hall was available for making measurements inside when the weather made in situ measurements impossible. The space was darkened to minimise the diffuse light to be negligible compared with the lamp.

2.3. Measurements

Three setups were used for the measurements.

- (1) Outside using sunlight when available. But since sunshine was frequently obstructed by clouds and trees:
- (2) outside using lamp. But since measurements were limited to dry nights only:
- (3) inside using lamp.

The measurements were normalized using a Labsphere Spectralon white reference panel. Outside, the target received light not only from the sun directly but scattered by sky, clouds, trees, and other environment. This diffuse component was measured separately by shading the direct sunlight using a thick screen.

The measurement sequence was as follows

- (1) Select azimuth (0°, 15°, 30°, 60°, 120°, 175°).
- (2) Normalize with the reference panel at nadir.
- (3) If outside, measure diffuse light.
- (4) Measure the spectra by varying the zenith angle [0°, 10°, ..., 70°, 0°].
- (5) Check the incident light level using the reference panel.
- (6) Select the next azimuth, illumination angle, or target.

Measurement for one azimuthal angle (items 2–5 above) usually took between 3 and 5 min and the whole hemisphere between 30 min and 1 h.

The targets were cleared of litter, cones, grass, and loose branches but otherwise left untouched. Some surrounding trees were cut down to allow more sunlight into the understory samples. The samples were carefully selected to be as clean, pure, and homogeneous as possible, hence

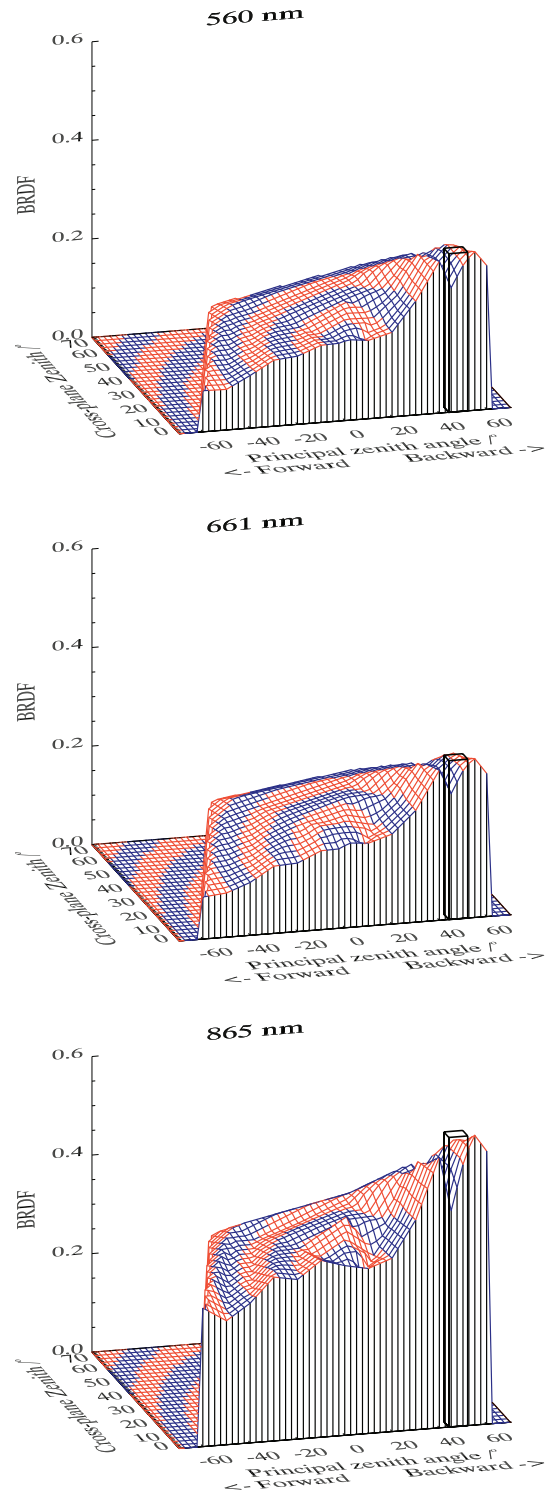


Fig. 4. The BRDF of lichen in three wavelengths (560, 661, and 865 nm). Lamp zenith angle is 48°, shown in the plot as a pillar. The concentric colored rings clarify zenith angles.

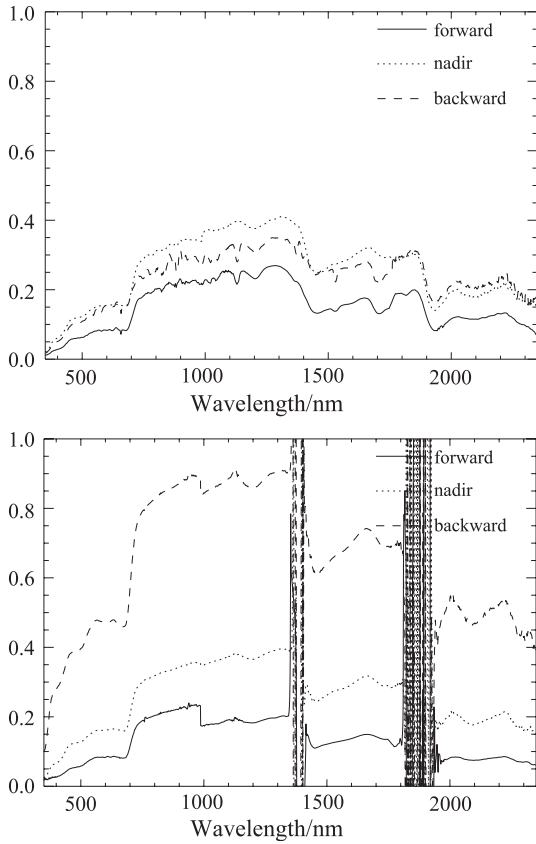


Fig. 5. The spectra of lichen in three directions: 50° forward, nadir and 50° backward in principal plane. Lamp zenith angle is 38° top and solar zenith angle is 62° bottom.

possibly not the most typical of the conditions in the area. For inside measurements, the samples were carefully dug from the ground using shovels and excavator and transported in as one big block weighing several hundreds of kilograms, retaining the surface in its original state.

The lichen sample consisted mainly of reindeer lichen (*Cladina rangiferina* and *C. stellaris*; Fig 3). The height of lichen was about 6 cm. The other species were moss (*D. polysetum*) and lingonberry, but the center was practically pure lichen. The moss sample was almost pure *D. polysetum* (Fig 3). Most pine needles were cleaned away from the center of the sample. The heather sample was about 20 cm tall, 60 twigs/m². There was also an abundance of lingonberry of 5–8 cm, about 50 twigs/m², and a continuous moss matt below (*D. polysetum*). Crowberry twigs were about 18 cm tall, and the density was about 150 twigs/m². The twigs were green from 8 cm height to top. The bottom was mainly moss (*D. polysetum*). Lingonberry plants covered about half of the sample. The mean height was 10 cm, varying from 6 to 12 cm. The bottom was moss (*D. polysetum*). Blueberry was about 16 cm tall, with a density of about 160 twigs/m². The sample also contained some lingonberry of 5–8 cm (about 100 twigs/m²). The bottom was mostly moss (*D. polysetum*). The mixed sample consisted of several dwarfs: heather (15%), lingonberry (30%), bearberry (30%), crowberry (15%), and hay

(*Agrostis* sp.; 10%) The dwarfs were 10–18 cm tall, the hays about 40 cm. The bottom was moss (*Polytrichum commune*).

3. Results

More than 2000 spectra were measured from seven targets in various directions. From outside measurements,

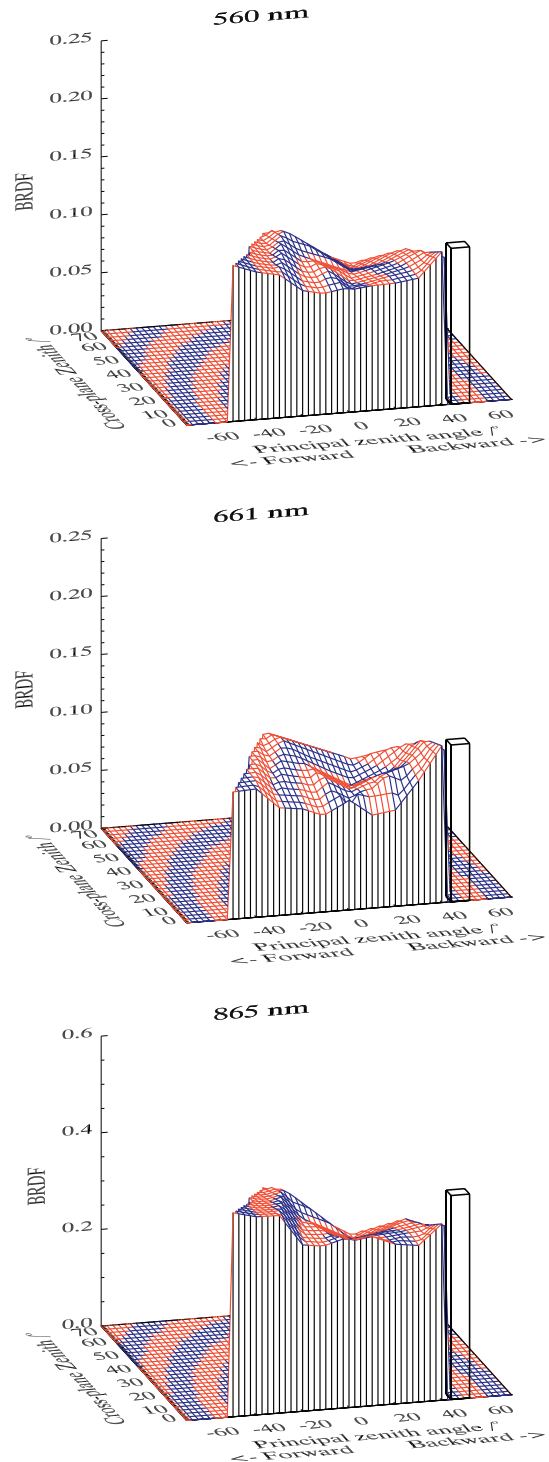


Fig. 6. The BRDF of moss as in Fig. 4.

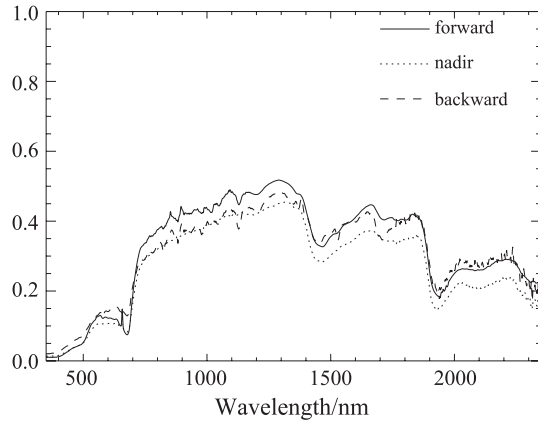


Fig. 7. The spectra of moss ($0^\circ, \pm 40^\circ$). Lamp zenith angle is 48° .

the diffuse light component (I_{diff}) was subtracted from full light (sun+diffuse) measurement (I)

$$R = \frac{I - I_{\text{diff}}}{I - I_{\text{stdiff}}}, \quad (2)$$

where I_{stdiff} is the measured intensity of the reference standard at diffuse light.

The results show large differences between species and some smaller variations between samples within the same species. For each target, a sample 3D BRDF diagram is presented at one to two illumination angles and at three wavelengths: green 560 nm, red 661 nm, and near-infrared 865 nm, all close to MERIS, MODIS, POLDER, and MISR bands. Additionally, full spectra in the range of 350–2350 nm are shown at three observation directions in the principal plane: backward (50° zenith angle), nadir, and forward (50°). The spectra measured at sunlight contain very much noise around 1390 and 1880 nm because all the light is absorbed by atmospheric water vapor. Sometimes, a discontinuity occurs at about 990 and 1770 nm because the spectrometer has three sensors, and each sensor sees a slightly different area of the inhomogeneous target (Table 1).

3.1. Lichen

Lichen (*Cladina arbuscula* and *C. rangiferina*) appeared to be a strong monotonic backward scatterer at all wavelengths (Figs. 4 and 5). The directional effect was stronger in visible, where the reflectivity is lower, and weaker in NIR, where the reflectivity is higher. There was no bowl shape typical of vegetation and soil. The spectrum was clearly grey and brighter in visible than that of green vegetation. The measured BRDFs look similar to those in Solheim et al. (2000).

3.2. Moss

Moss (*D. polysetum*) scattered relatively isotropically (within 20%) with some bowl shape in the visual bands and slightly forward in the NIR bands, contrary to lichen (Fig. 6). The spectrum was greener than that of lichen but lacked the yellow

absorption surge (Fig. 7). Solheim et al. (2000) also observed a flatter BRDF shape with *Racomitrium lanuginosum* moss but no forward scattering, which appeared in our measurements.

3.3. Heather and crowberry

Heather (*C. vulgaris*) was a strong backscatterer at all wavelengths (Figs. 8–10). The scattering pattern for

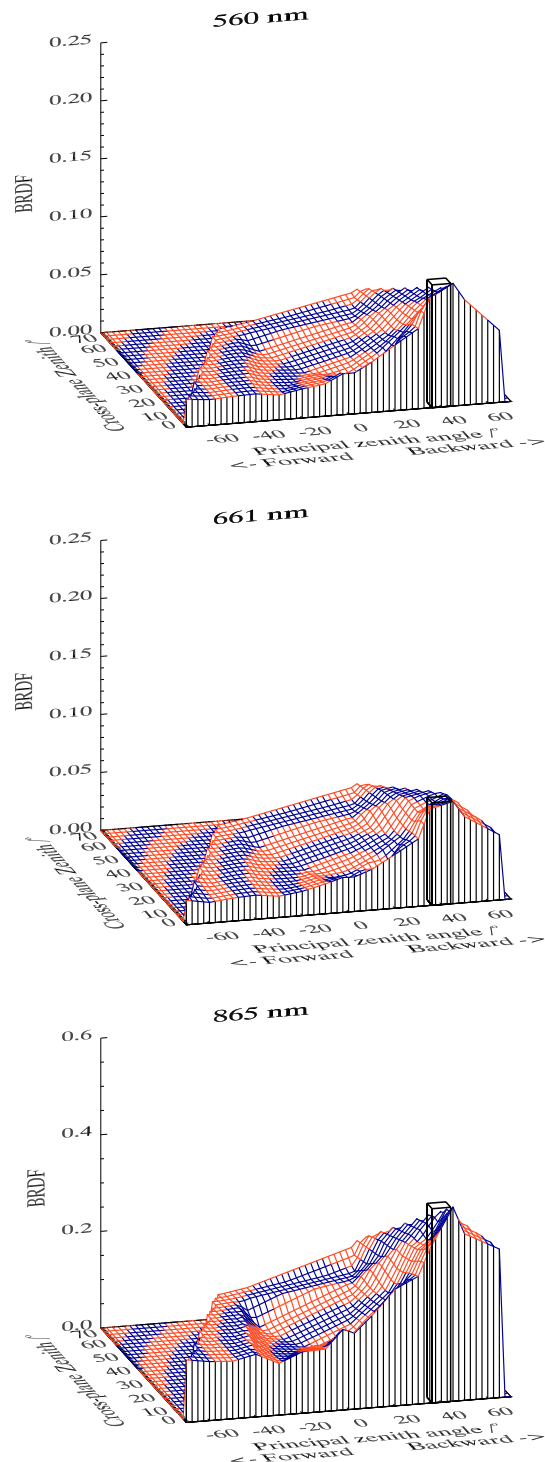


Fig. 8. The BRDF of heather as in Fig. 4. Lamp zenith angle is 40° .

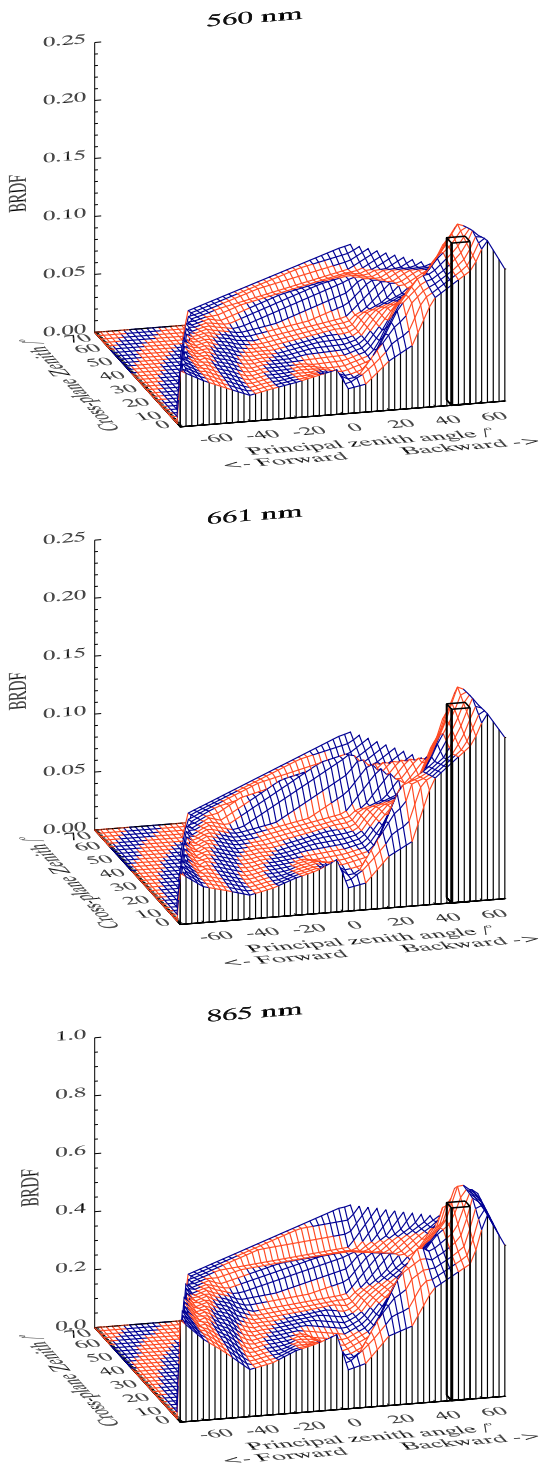


Fig. 9. The BRDF of heather 2 in sunlight as in Fig. 4. Solar zenith angle is 51°.

crowberry was similar but a little smoother (Fig. 11). A stronger bowl shape (sideways scattering) was observed for both heather and crowberry than for lichen or moss. Small forward enhancement was seen at lower solar illumination (i.e., larger phase angles). The same sample was remeasured after 3 days, and the results did not change significantly. Another heather sample was measured outside in sunlight,

and the result agreed well in qualitative level, that is, the major features were reproduced, although some quantitative differences occurred.

3.4. Blueberry and lingonberry

Blueberry (*V. myrtillus*) and lingonberry (*V. vitis-idaea*) scattered strongly forward—especially compared to heather—in the visible bands (Figs. 12–17). The forward scattering enhancement, compared to nadir or backward, was rather gray, that is, all wavelengths brighten rather similarly. Backward enhancement was more wavelength-dependent.

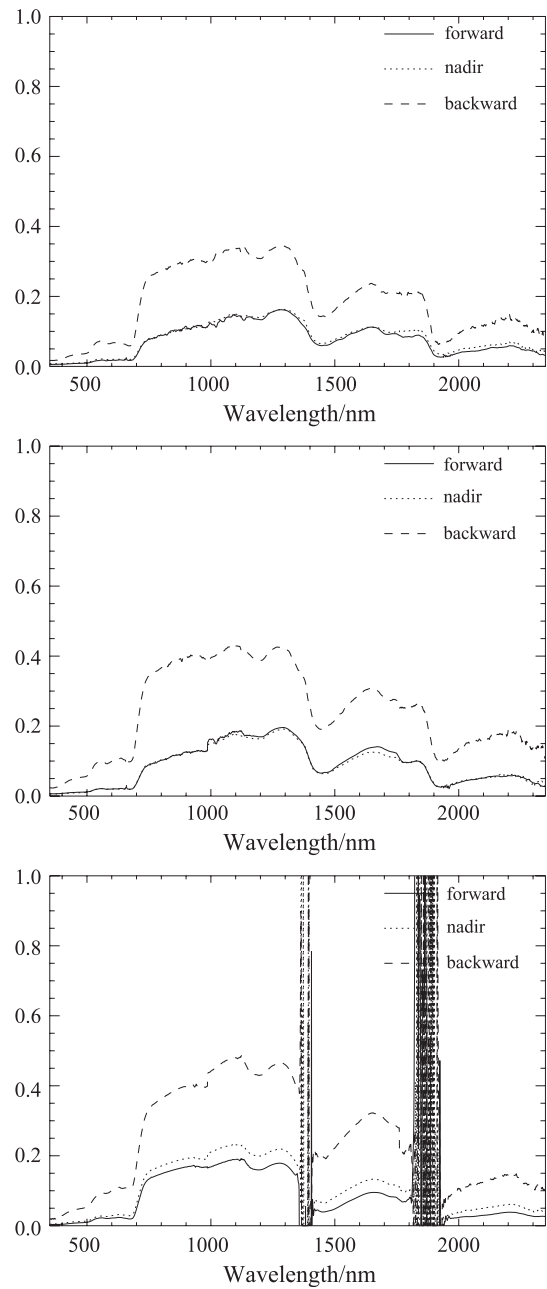


Fig. 10. The spectra of heather (0°, ±50°) 2×(0°, ±40°), Lamp zenith angles are 41° top and 50° middle, and solar zenith angle is 50° bottom.

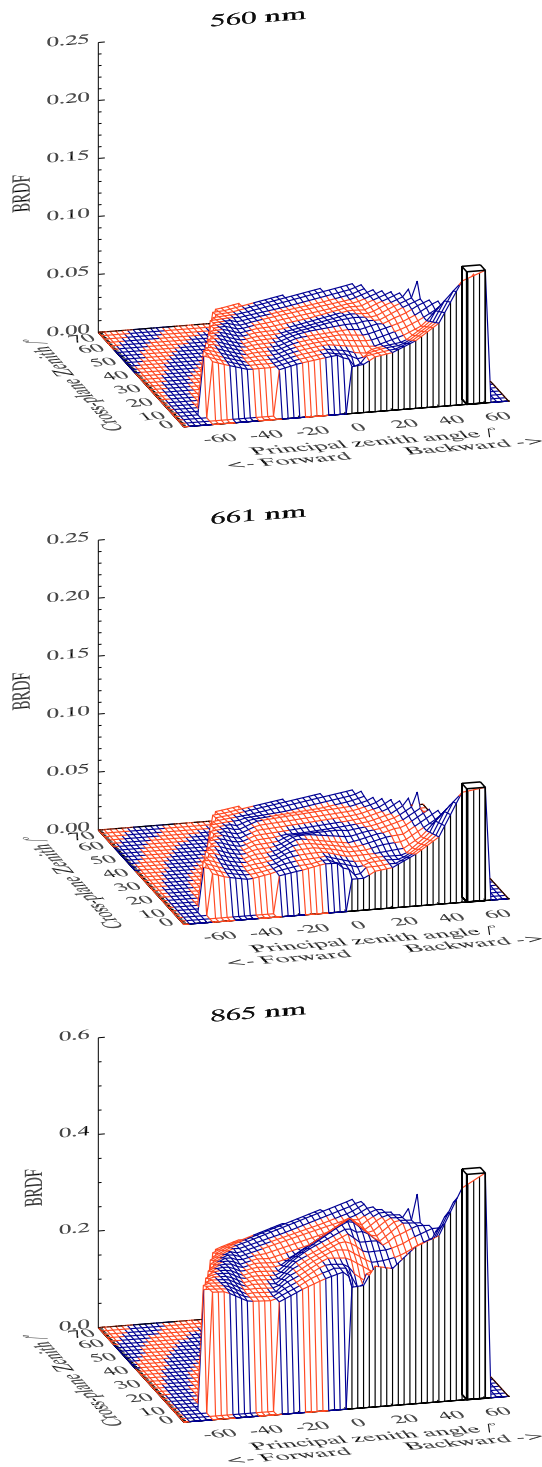


Fig. 11. The BRDF of crowberry as in Fig. 4. Solar zenith angle is 56°.

The scattering properties of individual leaves appear to dominate over geometrical and structural effects. The leaves have a waxy surface, causing significant specular reflection from their surface. In the visible spectral range, the light entering the inside of the leaves is mostly absorbed, but, in NIR, a large part is scattered diffusely, explaining the dramatic change in directional pattern.

3.5. Mixed understory

Finally, a mixed target that contained heather, blueberry, lingonberry, moss, grass, and litter was measured (Figs. 18–20). To get a better average, the target was measured from six points, about 15 cm apart, by moving the target between exposures. The standard deviation of the results was 15% averaged over all angles and 50% at forward

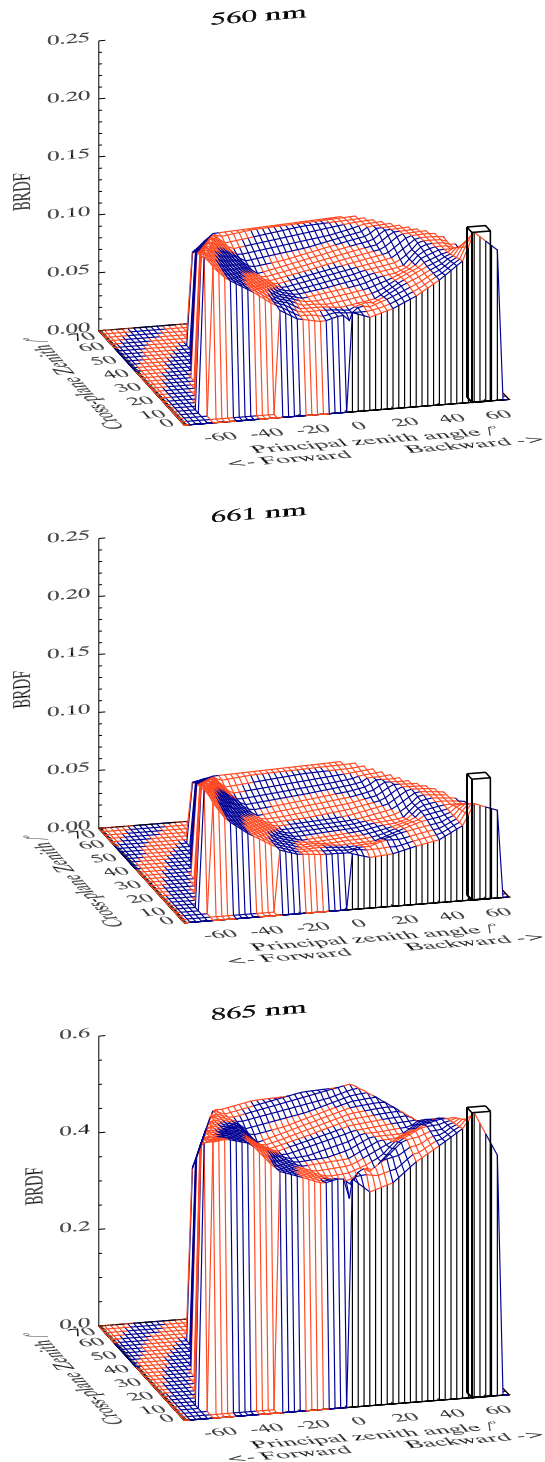


Fig. 12. The BRDF of blueberry as in Fig. 4. Lamp zenith angle is 58°.

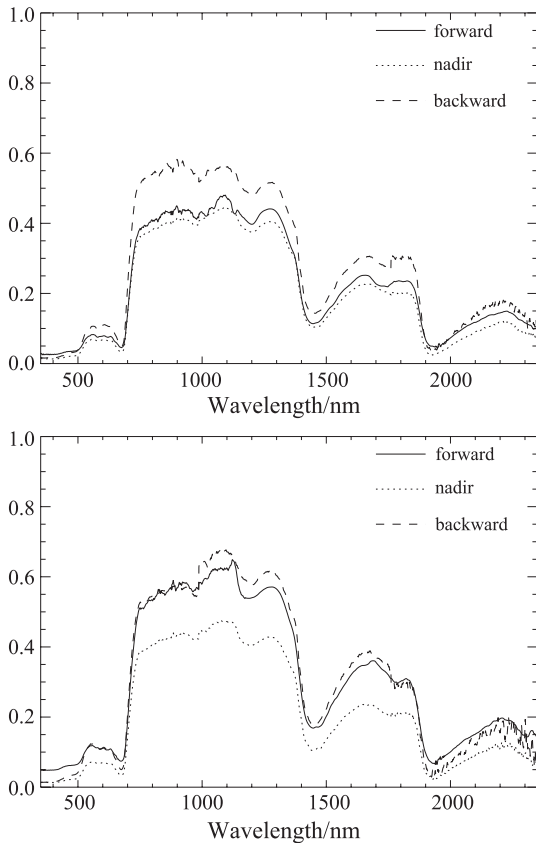


Fig. 13. The spectra of blueberry ($0^\circ, \pm 50^\circ$). Lamp zenith angles are 42° top and 58° bottom.

angles. The directional pattern, even after averaging over the six spots, was more noisy than with pure samples.

There was some forward scattering enhancement, but weaker than with lingonberry or blueberry, and rather much backscattering, but a little weaker than with heather.

4. Conclusions

A technique for measuring the BRDF of understory vegetation, both in situ and in the laboratory, is introduced.

BRDF of seven of the most typical species in Finnish pine forests is measured in one to three illumination conditions. The spectral and directional properties of the understory vary considerably. However, characteristic features are observable for all the species.

All targets have some signs of backscattering enhancement—heather and lichen the strongest, moss the weakest. Lingonberry and blueberry also scatter relatively strongly forward. In general, the directional features are significant and non-Lambertian, more striking at larger solar zenith angles than at smaller ones. The BRDF depends strongly on the wavelength. Separation of the causes of the effects (canopy structure or single leaf) needs further measurement.

The results provide input for physical reflectance models. Without any information on how much the over- and

understory vegetations contribute to the reflectance of a stand in given illumination and viewing conditions at a certain wavelength, it is not possible to separate the two components in a reliable way. For applications where quantitative undergrowth inversion is not needed, the type of data presented in this paper will probably give a sufficient lower boundary condition. For instance, if the relative

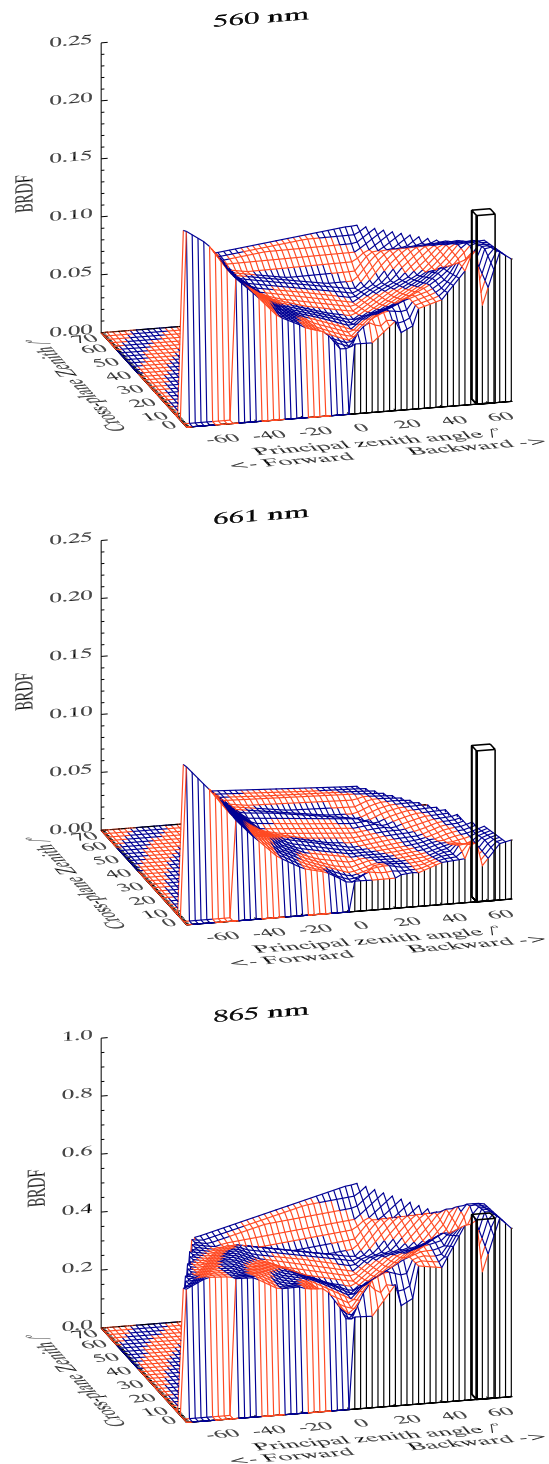


Fig. 14. The BRDF of lingonberry as in Fig. 4. Lamp zenith angle is 59° .

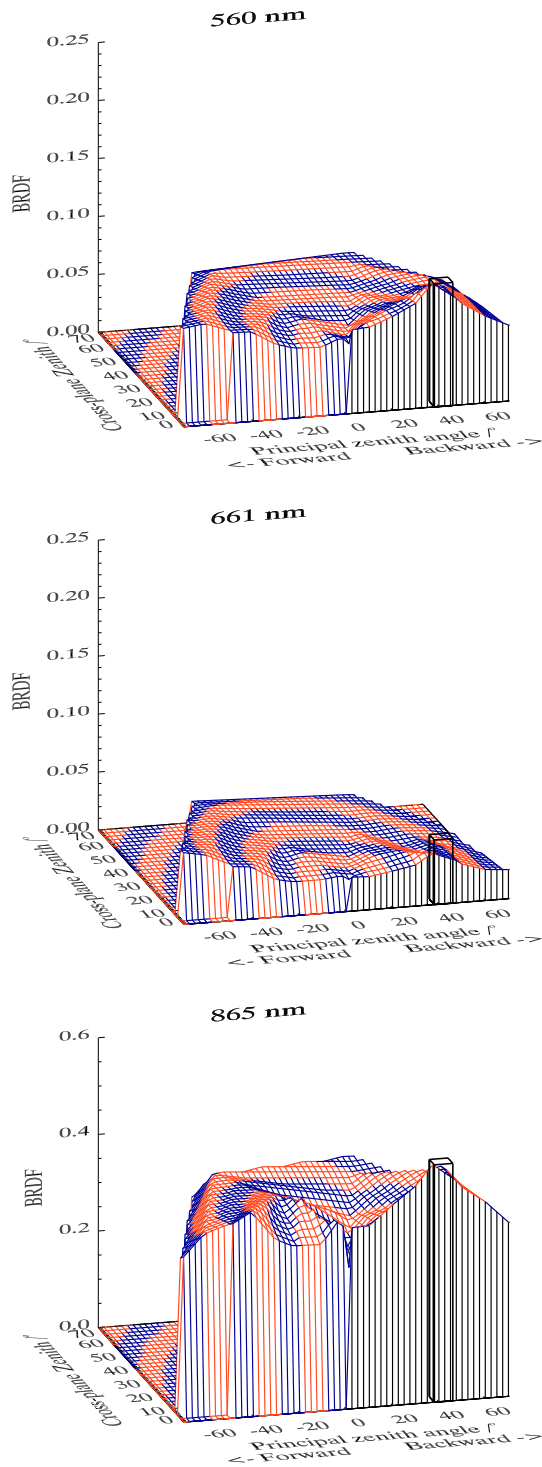


Fig. 15. The BRDF of lingonberry as in Fig. 4. Lamp zenith angle is 42°.

abundances of understory species are known, it is possible to define some mixing rules for obtaining the understory reflectance through, e.g., linear interpolation. However, all mixing is not linear, and there may be significant complications in nature.

The results appeared reproducible and consistent, but some possible sources of error remain. The inhomogeneous spot of the lamp caused some unrecoverable systematic

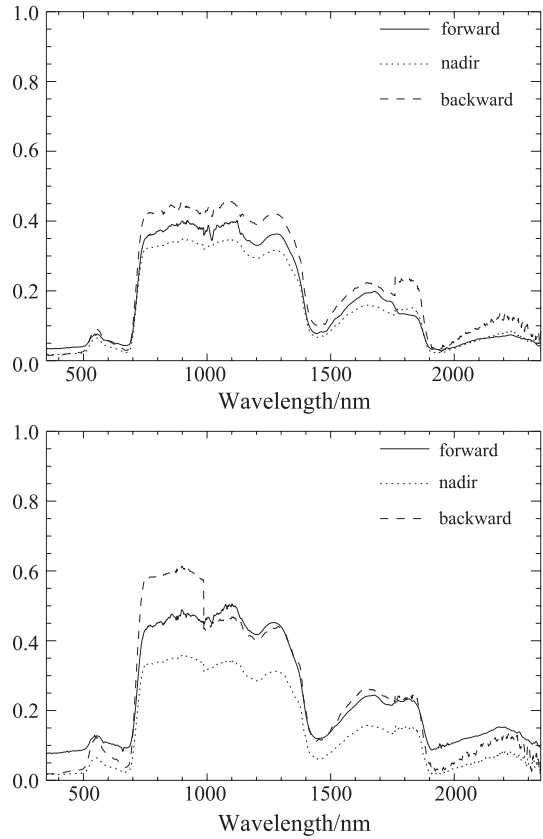


Fig. 16. The spectra of lingonberry (0°, ±50°). Lamp zenith angles 42° (top) and 59° (bottom).

error of the order of 10–30%. Outside, the variations of the sky were well below 10% when checked, but since there were no simultaneous monitoring of the skylight available, it is always possible that some unobserved short-term variations occurred. Some calibration errors may be caused by the reference standard getting dirty or having reflection properties changed from the original. Other instrumental errors are assumed negligible. Some variations in the data are caused by the detector footprint moving and elongating

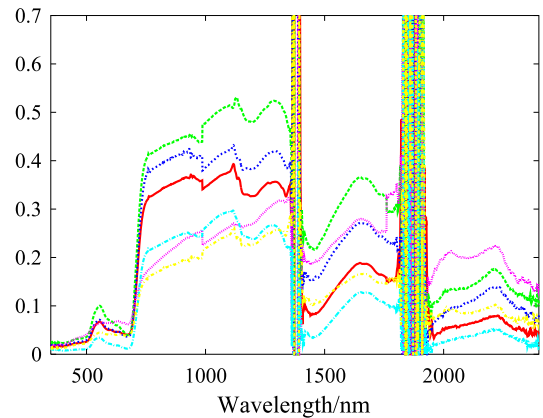


Fig. 17. A set of spectra of lingonberry measured at nadir and taken at various locations a few meters apart showing the large variations even among the same species.

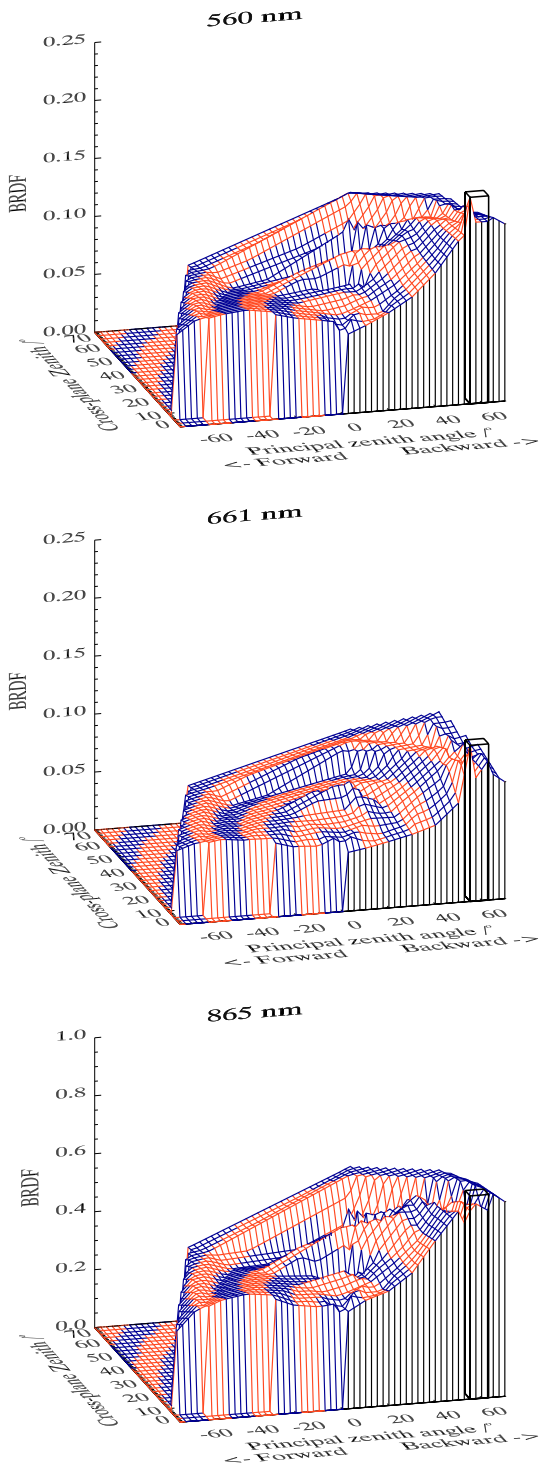


Fig. 18. The BRDF of mixed understory as in Fig. 4. Lamp zenith angle is 58°.

during the measurements. Compared to the large natural variations in the measured data, all these errors are significant only in detailed albedo comparisons.

Future measurements should focus on extending the angular range of the present measurements (more illumination angles, larger observation zenith angles, and back scattering), including new targets, and studying more

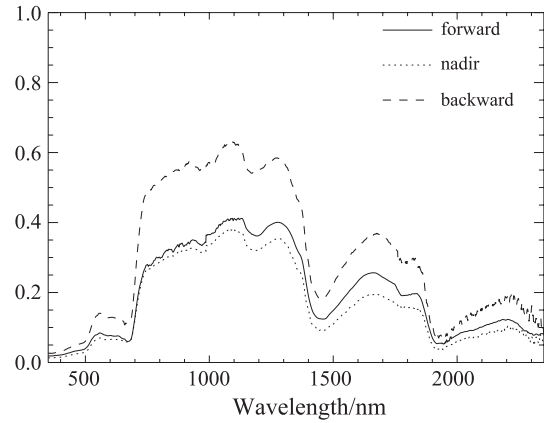


Fig. 19. The spectra of mixed understory (0°, ±50°). Lamp zenith angle is 58°.

systematically the sensitivity of the scattering features on specific physical properties of the targets, e.g., moisture, diurnal and seasonal variations, structural parameters, leaf properties, and underlying soil. Separate measurements of single leaf scattering will help with modeling and interpreting the measurements. Topics of future research are albedo comparisons, parametrisations, and applications.

The measurements also led to improved instrumentation. Based on the experience, a new lamp system with a smooth stable spectrum and flat spot was constructed, and a new automatic portable field goniometer was developed.

Acknowledgments

Sanna Kaasalainen’s work is funded by the Academy of Finland. The work of Rautiainen and Stenberg has been supported by the Foundation for Research of Natural Resources in Finland and Tekes, The National Technology Agency Finland (ENBOR2).

Anonymous reviewers are thanked for valuable comments.

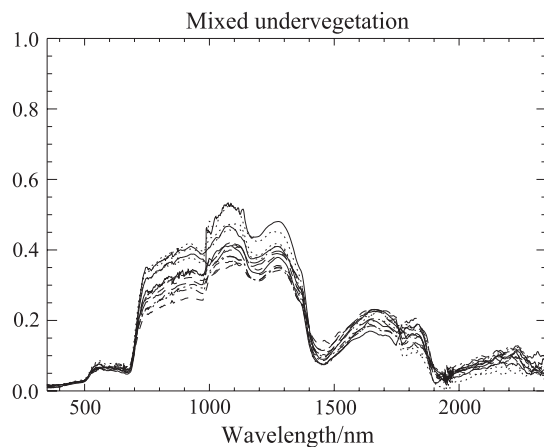


Fig. 20. A set of spectra (at nadir) of the mixed understorey target taken at various locations a few centimeters apart showing the large variations in natural samples.

References

- Bonnefoy, N., Brissaud, O., Schmitt, B., Douté, S., Fily, M., Grundy, W., et al. (2000). Experimental system for the study of planetary surface materials' BRDF. *Remote Sensing Reviews*, 19(1–4), 59–74.
- Brissaud, O., Schmitt, B., Bonnefoy, N., Rabou, S. D. P., Grundy, W., & Fily, M. (2004). Spectrogonio radiometer for the study of the bidirectional reflectance and polarization functions of planetary surfaces: 1. Design and tests. *Applied Optics*, 43, 1926–1937.
- Bruegge, C. J., Helmlinger, M. C., Conel, J. E., Gaitley, B. J., & Abdou, W. A. (2000). PARABOLA III: A sphere-scanning radiometer for field determination of surface anisotropic reflectance functions. *Remote Sensing Reviews*, 19(1–4), 75–94.
- Chen, J. M., & Cihlar, J. (1996). Retrieving leaf area index of boreal conifer forests using Landsat TM images. *Remote Sensing of Environment*, 55, 153–162.
- Dawson, T., Curran, P., & Plummer, S. (1998). LIBERTY—modeling the effects of leaf biochemical concentration on reflectance spectra. *Remote Sensing of Environment*, 65(1), 50–60.
- Demircan, A., Geiger, B., Radke, M., & von Schönemark, M. (2000). Bidirectional reflectance measurements with the CCD line camera WAAC. *Remote Sensing Reviews*, 19(1–4), 95–110.
- Ganapol, B., Johnson, L., Hammer, P., Hlavka, C., & Peterson, D. (1998). LEAFMOD: A new within-leaf radiative transfer model. *Remote Sensing of Environment*, 63(2), 182–193.
- Hapke, B. (1993). *Theory of reflectance and emittance spectroscopy*. Cambridge University Press.
- Hosgood, B., Sandmeier, S., Piironen, J., Andreoli, G., & Koechler, C. (2000). Goniometers. In J. Webster (Ed.), *Encyclopedia of Electronics Engineering*, vol. 8 (pp. 424–433) New York: John Wiley.
- Huete, A. (1989). Soil influences in remotely sensed vegetation–canopy spectra. In G. Asrar (Ed.), *Theory and applications of optical remote sensing* (pp. 107–141). John Wiley and Sons.
- Jacquemoud, S., & Baret, F. (1990). PROSPECT: A model of leaf optical properties spectra. *Remote Sensing of Environment*, 34, 75–91.
- Jacquemoud, S., Baret, F., & Hanocq, J. F. (1992). Modeling spectral and bidirectional soil reflectance. *Remote Sensing of Environment*, 41, 123–132.
- Kaufman, Y. (1989). The atmospheric effect on remote sensing and its corrections. In G. Asrar (Ed.), *Theory and applications of optical remote sensing* (pp. 336–428). John Wiley and Sons.
- Kuusk, A. (1991). The angular distribution of reflectance and vegetation indices in barley and clover canopies. *Remote Sensing of Environment*, 37, 143–151.
- Kuusk, A. (2001). A two-layer canopy reflectance model. *Journal of Quantitative Spectroscopy & Radiative Transfer*, 71(1), 1–9.
- Kuusk, A., & Nilson, T. (2000). A directional multispectral forest reflectance model. *Remote Sensing of Environment*, 72, 244–252.
- Lang, M., Kuusk, A., Nilson, T., Lukk, T., Pehk, M., & Alm, G. (Accessed May 2 2002). Reflectance spectra of ground vegetation in sub-boreal forests. web page. available on-line [<http://www.aai.ee/bgf/ger2600/>].
- Li, X., Strahler, A., & Woodcock, C. (1995). A hybrid geometric optical–radiative transfer approach for modelling albedo and directional reflectance of discontinuous plant canopies. *IEEE Transactions on Geoscience and Remote Sensing*, 33, 466–480.
- Liang, S. (2004). *Quantitative remote sensing of land surfaces. Wiley series in remote sensing*. New Jersey: Wiley.
- North, P. (1996). Three-dimensional forest light interaction model using a Monte Carlo method. *IEEE Transactions on Geoscience and Remote Sensing*, 34, 946–956.
- Peltoniemi, J., Kaasalainen, S., Näränen, J., Matikainen, L., & Piironen, J. (2004). The measurement of directional and spectral signatures of light reflectance by snow. *IEEE Transactions on Geoscience and Remote Sensing* (Submitted for publication).
- Rees, W., Tutubalina, O., E., & G. (2004). Reflectance spectra of subarctic lichens between 400 and 2400 nm. *Remote Sensing of Environment*, 90(3), 281–292.
- Sandmeier, S. R., & Itten, K. I. (1999). A field goniometer system (FIGOS) for acquisition of hyperspectral BRDF data. *IEEE Transactions on Geoscience and Remote Sensing*, 37, 648–658.
- Solheim, I., Engelsen, O., Hosgood, B., & Andreoli, G. (2000). Measurement and modeling of the spectral and directional reflection properties of lichen and moss canopies. *Remote Sensing of Environment*, 72, 78–94.
- Spanner, M., Pierce, L., Peterson, D., & Running, S. (1990). Remote sensing of temperate coniferous leaf area index: The influence of canopy closure, understory vegetation, and background reflectance. *International Journal of Remote Sensing*, 11(1), 95–111.
- Strub, G., Schaepman, M., Knyazikhin, Y., & Itten, K. (2003, May). Evaluation of spectro-directional alfalfa canopy data acquired during DAISEX'99. *IEEE Transactions on Geoscience and Remote Sensing*, 41(5), 1034–1042.
- Walter-Shea, E., & Norman, J. (1991). Leaf optical properties. In R. Myneni, & J. Ross (Eds.), *Photon–vegetation interactions: Applications in optical remote sensing and plant ecology* (pp. 229–251). Berlin: Springer-Verlag.
- Widlowski, J. -L., Pinty, B., & Gobron, N. (2001). Detection and characterization of boreal coniferous forests from remote sensing data. *Journal of Geophysical Research*, 106(D24), 33405–33419.